



Full dimensional quantum dynamics study of isotope effects for the $\text{H}_2 + \text{NH}_2 / \text{ND}_2 / \text{NHD}$ and $\text{H}_2 / \text{D}_2 / \text{HD} + \text{NH}_2$ reactions

Zhang Donghui, Xiaoren Zhang, Zhaojun Zhang, Fabien Gatti, Dong Zhang

► To cite this version:

Zhang Donghui, Xiaoren Zhang, Zhaojun Zhang, Fabien Gatti, Dong Zhang. Full dimensional quantum dynamics study of isotope effects for the $\text{H}_2 + \text{NH}_2 / \text{ND}_2 / \text{NHD}$ and $\text{H}_2 / \text{D}_2 / \text{HD} + \text{NH}_2$ reactions. The Journal of Chemical Physics, 2021, 154 (7), pp.074301. 10.1063/5.0040002. hal-03064558

HAL Id: hal-03064558

<https://hal.science/hal-03064558>

Submitted on 18 Feb 2021

HAL is a multi-disciplinary open access archive for the deposit and dissemination of scientific research documents, whether they are published or not. The documents may come from teaching and research institutions in France or abroad, or from public or private research centers.

L'archive ouverte pluridisciplinaire **HAL**, est destinée au dépôt et à la diffusion de documents scientifiques de niveau recherche, publiés ou non, émanant des établissements d'enseignement et de recherche français ou étrangers, des laboratoires publics ou privés.

Full dimensional quantum dynamics study of isotope effects for the $\text{H}_2+\text{NH}_2/\text{ND}_2/\text{NHD}$ and $\text{H}_2/\text{D}_2/\text{HD}+\text{NH}_2$ reactions

Xiaoren Zhang^{1,2}, Zhaojun Zhang^{1, a)}, Fabien Gatti^{3, b)} and Dong H. Zhang^{1c)}

¹*State Key Laboratory of Molecular Reaction Dynamics and Center for Theoretical and Computational Chemistry, Dalian Institute of Chemical Physics, Chinese Academy of Sciences, Dalian 116023, P.R. China;*

²*University of Chinese Academy of Sciences, Beijing 100049, China;*

³*ISMO, Institut des Sciences Moléculaires d'Orsay - UMR 8214 CNRS/Université Paris-Saclay, F-91405 Orsay, France*

A full dimensional quantum dynamical study for the bimolecular reactions of hydrogen molecule with amino radical for different isotopologues is reported. The nonreactive amino radical is described by two Radau vectors that are very close to the valence bond coordinates. Potential optimized discrete variable representation basis is used for the vibrational coordinates of amino radical. Starting from the reaction H_2+NH_2 , we study the isotope effects for the two reagents separately, i.e., $\text{H}_2+\text{NH}_2/\text{ND}_2/\text{NHD}$ and $\text{H}_2/\text{D}_2/\text{HD}+\text{NH}_2$. The effects of different vibrational modes excitations of the reagents on the reactivities are studied. Clear explanations about the isotope effects are also provided thoroughly including the influence of vibrational energy differences between the different isotopologues and the impact of tunneling effect.

^{a)}E-mail: zhangzhj@dicp.ac.cn

^{b)}E-mail: fabien.gatti@u-psud.fr

^{c)}E-mail: zhangdh@dicp.ac.cn

I. INTRODUCTION

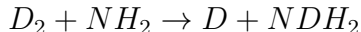
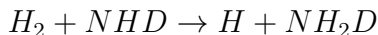
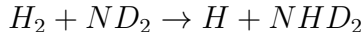
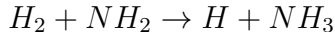
$\text{H}+\text{NH}_3 \leftrightarrow \text{H}_2+\text{NH}_2$ is the simplest five atomic reaction and plays a significant role in the combustion of ammonia. During the last two decades, after a long focus on molecular systems with three or four atoms^{1–13}, scientists began to extend the full quantum-mechanical studies to molecular systems with more than four atoms in reduced dimensionality^{14–27} or full dimensionality^{28–39}. As a result, the title pentaatomic reaction and its isotopically substituted analogs serves as a benchmark to develop various quantum mechanical methods.

Compared to the reaction $\text{H}+\text{NH}_3 \rightarrow \text{H}_2+\text{NH}_2$, the reverse reaction H_2+NH_2 was seldom studied. In 2007, Yang et.al. developed a seven dimensional model for the H_2+NH_2 reaction in which the nonreactive NH_2 group keeps a C_{2v} symmetry and the rotation-vibration coupling in NH_2 was neglected. Their calculations were carried out using an analytical potential energy surface (PES) developed by Corchado and Espinosa-García, which accuracy was not sufficient enough. In 2014, a more accurate PES was constructed by Li and Guo (LG) using the permutation-invariant polynomial neural network (PIP-NN) method. They used more than 100,000 ab initio geometries at the UCCSD(T)-F12a/aug-cc-pVTZ level of theory and the fitting error of the PES was very small. Later on, Song et.al. performed a full dimensional quantum dynamics calculations on this PES. In their model, a description in purely Jacobi coordinates was adopted. Influence of the excitation of the different vibrational modes and the rotation on the $\text{H}_2+\text{NH}_2 \rightarrow \text{H}+\text{NH}_3$ reaction have been examined in detail. In their calculations, the integral cross sections for most initial states were obtained using the so-called J-shifting (JS) approximation to reduce the expensive computational cost.

In the past several years, accurate quantum studies for the chemical elemental reaction involving five and six atoms have been made very significant progresses^{28–39}. Our groups adopted a description of Jacobi-Radau mixed polyspherical coordinates, which proved to be efficient to deal with polyatomic systems such as $\text{H}+\text{NH}_3$ ⁴⁰ and $\text{H}+\text{CH}_4$ ⁴¹. During the reaction processes, certain parts of the molecular systems do not display motions of large amplitude and move around a specific symmetry. Therefore, a subsystem strategy can be easily implemented to study those reactions. As have been shown in our previous papers for the reactions $\text{H}+\text{NH}_3$ ⁴⁰ and $\text{H}+\text{CH}_4$ ⁴¹, the nonreactive groups NH_2 and CH_3 do not change dramatically and thus can be both described using Radau coordinates, which are close to the valence internal coordinates. While the Jacobi coordinates are used only for the bond breaking and creating. Using these Jacobi and Radau mixed

coordinates along with a potential-optimized discrete variable representation (PODVR)^{42,43} even for the angular degree of freedoms can thus be applied. Consequently, a smaller number of basis functions is sufficient for the scattering calculations. For the first time, we carried out full dimensional quantum studies for the $\text{H}+\text{CH}_4 \rightarrow \text{H}_2+\text{CH}_3$ system using time independent basis functions. This allowed us to shed light on the physics of these elementary reactions and also to demonstrate the efficiency of our description in mixed Jacobi/Radau coordinates combined with a PODVR approach for quantum scattering of reactions with 5 and 6 atoms.

In this field, isotope effects are often of great importance. In general, the change of the density of the energy levels as well as the difference of the tunneling effects can all be attributed to isotope (i.e. mass) effects. This is the reason why, to provide a detailed insight in the isotope effects for the bimolecular reaction H_2+NH_2 , we study here the following five reactive systems in full dimensionality:



In our present method the nonreactive moiety amino molecular $\text{NH}_2/\text{ND}_2/\text{NHD}$ is described using two Radau vectors⁴⁴⁻⁴⁶ while the bond breaking and formation are described by two Jacobi vectors. As aforementioned, this mixed coordinates have proven to be successful method in dealing with polyatomic systems especially with systems involving five or six atoms. In the above reactions, there exist indeed a nonreactive subgroup $\text{NH}_2/\text{ND}_2/\text{NHD}_2$ in which there is no motion of large amplitude. Compared to a description in Jacobi coordinates only, the fact that we use Radau coordinates for the ‘semi-rigid’ subgroup allows us to save basis set functions as have already shown in our previous studies. PODVR basis functions are then used for the three vibrational degrees of freedom including one angle and two radial coordinates for the nonreactive group $\text{NH}_2/\text{ND}_2/\text{NHD}$.

This paper is organized as follows. Section II gives the definition of the coordinates and the kinetic energy operator for the reaction system $\text{XY}+\text{NZ}_{1,2}$, as well as a brief description of the basis functions and time-dependent method. In section III, results and discussions for the five reactions are presented in detail. A brief summary (section IV), concludes the paper.

II. THEORY

The coordinates used to describe the XY+NZ_{1,2} systems are depicted in Fig. 1: they combine two Jacobi vectors (\vec{R}, \vec{r}) with two Radau vectors (\vec{R}_1, \vec{R}_2). These vectors are parametrized in terms of spherical coordinates and correspond to a particular case of the so-called family of polyspherical coordinates^{47–49}. More specifically, we use a separation into two subsystems⁵⁰ with two Radau coordinates for the molecule NZ_{1,2} (similar to the approach in Ref.⁴⁶) and one subsystem with one Jacobi vector for XY. Since we use standard polyspherical approach, the z Body-Fixed axis for the NZ_{1,2} is parallel to one of the two Radau vectors and the kinetic energy operator (KEO) can then been straightforwardly derived from the polyspherical formulation.

The Radau vectors^{44–46} \vec{R}_i ($i=1,2$) are the vectors $\overrightarrow{AZ_i}$ with A the “canonical” point of NZ_{1,2} defined as the geometric mean of NG_{Z_{1,2}} and G_{NZ_{1,2}}G_{Z_{1,2}}. Here, N refers to the N-atom, G_{NZ_{1,2}} is the center of mass of NZ_{1,2}, G_{Z_{1,2}} is the center of mass of the Z_{1,2} group. More precisely, the canonical point is defined by $(AG_{Z_{1,2}})^2 = G_{NZ_{1,2}}G_{Z_{1,2}} \times NG_{Z_{1,2}}$. If we define $\vec{r}_i = \overrightarrow{G_{NZ_{1,2}}Z_i}$ ($i = 1, 2$), the Radau vectors will have the following form:

$$\begin{aligned}\vec{R}_1 &= (1 - \alpha m_{Z_1})\vec{r}_1 - \alpha m_{Z_2}\vec{r}_2, \\ \vec{R}_2 &= -\alpha m_{Z_1}\vec{r}_1 + (1 - \alpha m_{Z_2})\vec{r}_2,\end{aligned}\tag{1}$$

with

$$\alpha = (1 - \sqrt{\frac{M}{m_N}})/m_{Z_{1,2}},\tag{2}$$

and $m_{Z_{1,2}} = m_{Z_1} + m_{Z_2}$, $M = m_N + m_{Z_{1,2}}$.

The Jacobi vector, \vec{R} , is the vector from the center of mass of NZ_{1,2} to the center of mass of XY molecular, and \vec{r} is from Y atom to X atom. Therefore, the hamiltonian for the XY+NZ_{1,2} reaction system can be written as ($\hbar = 1$),

$$\begin{aligned}\hat{H} &= -\frac{1}{2\mu_R}\frac{\partial^2}{\partial R^2} + \frac{(\vec{J}_{tot} - \vec{J}_{12})^2}{2\mu_R R^2} - \frac{1}{2\mu_r}\frac{\partial^2}{\partial r^2} + \frac{\vec{J}_1^2}{2\mu_r r^2} + \hat{T}_{NZ_{1,2}} \\ &\quad + V(R, r, \theta_1, \theta_2, \varphi_1, \varphi_2, R_1, R_2, \theta),\end{aligned}\tag{3}$$

in which

$$\mu_R = \frac{(m_X + m_Y)m_{NZ_{1,2}}}{m_X + m_Y + m_N + m_{Z_1} + m_{Z_2}},\tag{4}$$

$$\mu_r = \frac{m_X m_Y}{m_X + m_Y}.\tag{5}$$

where \vec{J}_{tot} is the total angular momentum operator of the system, \vec{j}_1 is the rotational angular momentum operator of XY, \vec{j}_{12} is the coupling angular momentum operator of \vec{j}_1 and the rotational angular momentum operator \vec{j}_2 of $NZ_{1,2}$. V denotes the potential energy surface. If we define $u = \cos \theta$, $u_1 = \cos \theta_1$ and $u_2 = \cos \theta_2$, the (non-Euclidean for the lengths of the vectors) volume element reads:

$$dV = dR dr du_1 du_2 d\varphi_1 d\varphi_2 dR_1 dR_2 du. \quad (6)$$

For the KEO of $T_{NZ_{1,2}}$, one can refer our previous papers^{40,49} for more information. The $T_{NZ_{1,2}}$ contains three parts,

$$\hat{T}_{NZ_{1,2}} = \hat{T}_{vib} + \hat{T}_{rot} + \hat{T}_{cor}. \quad (7)$$

The vibrational parti reads:

$$2\hat{T}_{vib} = - \sum_{i=1,2} \frac{1}{\mu_i} \frac{\partial^2}{\partial R_i^2} - \left(\frac{1}{\mu_1 R_1^2} + \frac{1}{\mu_2 R_2^2} \right) \frac{\partial}{\partial u} v^2 \frac{\partial}{\partial u}, \quad (8)$$

where $\mu_1 = m_{Z_1}$, $\mu_2 = m_{Z_2}$, $u = \cos \theta$ and $v = \sin \theta$.

The rotational part:

$$\begin{aligned} 2T_{rot} = & \vec{j}_{2z}^2 \left(\frac{1}{\mu_1 R_1^2 \sin^2 \theta} + \frac{\cot^2 \theta}{\mu_2 R_2^2} \right) + \frac{\vec{j}_2^2 - \vec{j}_{2z}^2}{\mu_2 R_2^2} \\ & + \frac{\cot \theta}{\mu_2 R_2^2} (\vec{j}_{2x} \vec{j}_{2z} + \vec{j}_{2z} \vec{j}_{2x}). \end{aligned} \quad (9)$$

The ‘‘coriolis’’ coupling part:

$$2T_{cor} = \vec{j}_{2y} \frac{\sin \theta}{\mu_2 R_2^2} P_u + P_u \frac{\sin \theta}{\mu_2 R_2^2} \vec{j}_{2y}. \quad (10)$$

In time dependent wave packet methods, the wavefunction for the scattering calculation can be expanded as

$$\begin{aligned} \Psi(\vec{R}, \vec{r}, \vec{R}_1, \vec{R}_2, t) = & \sum_{n\nu_1\nu_2j} F_{n\nu_1\nu_2j} u_n^{\nu_r}(R) \\ & \times \phi_{\nu_r}(r) \phi_{R_1}(R_1) \phi_{R_2}(R_2) \phi_{\theta}(\theta) Y_j^{J_{tot}MK}(\vec{R}, \vec{r}, \vec{R}_1, \vec{R}_2), \end{aligned} \quad (11)$$

where n labels the translational basis, j denotes $(j_1 j_2 j_{12} k)$.

The rotational basis functions for the XY+NZ_{1,2} system in the body-fixed frame can be written as

$$Y_j^{J_{tot}MK} = \sum_m \langle j_1 m j_2 K - m | j_{12} K \rangle Y_{j_1 m}(\vec{r}) \bar{D}_{K-mk}^{j_2}(\vec{R}_1, \vec{R}_2), \quad (12)$$

where M and K are the projection of the total angular momentum J_{tot} on the z-axis of space-fixed and body-fixed frames, respectively. k is the projection of the rotational angular momentum j_2 on the z-axis of $NZ_{1,2}$ frame. $Y_{j_{1m}}(\vec{r})$ are the spherical harmonics for the XY molecule, $\bar{D}_{K-mk}^{j_2}(\vec{R}_1, \vec{R}_2)$ are the Wigner rotational matrices for the rotation of the $NZ_{1,2}$ molecule. They are defined as

$$Y_{j_{1m}}(\vec{r}) = Y_{j_{1m}}(\theta_1, \varphi_1), \quad (13)$$

$$\bar{D}_{K-mk}^{j_2}(\vec{R}_1, \vec{R}_2) = \sqrt{\frac{2j_2+1}{4\pi}} D_{K-mk}^{*j_2}(0, \theta_2, \varphi_2). \quad (14)$$

The initial wave packet is constructed as a product of a specific rovibrational eigenfunction ($\nu_{10}\nu_{20}j_{10}j_{20}j_{120}$) for reactants and a localized translational wave packet for R . The second-split operator method is used to propagate the wave packet⁵¹. As shown in our previous paper⁴¹, the time-independent wave functions will be calculated and the total reaction probability is calculated using the standard flux method at a dividing surface.

$$P_i(E) = \frac{\hbar}{\mu_r} \text{Im}(\langle \psi_{iE} | \psi'_{iE} \rangle) |_{r=r_s}, \quad (15)$$

where ψ'_{iE} the first derivative of the time-independent wave function in r .

To calculate the integral cross section for a specific initial state, one needs to sum the reaction probabilities over all the partial waves (total angular momentum J_{tot})

$$\sigma_{\nu_1\nu_2j_1j_2}(E) = \frac{1}{(2j_1+1)(2j_2+1)} \sum_{Kj_{12}} \left\{ \frac{\pi}{k_E^2} \sum_{J_{tot} \geq K} (2J_{tot}+1) P_{\nu_1\nu_2j_1j_2K}^{J_{tot}}(E) \right\}, \quad (16)$$

where $k_E = \sqrt{2\mu_R E}$. In this paper, the initial rotational quantum numbers j_1 and j_2 are restricted to zero. j_{12} is the sum of j_1 and j_2 and thus also equal to zero.

III. RESULTS AND DISCUSSIONS

In this work the PES employed for the scattering calculations was constructed by Li and Guo (LG) **Fabien: Ref.** This PES has been used for many dynamical calculations and the comparison with experimental data has proven that the PES is very accurate **Fabien: Ref.** To reduce the computational effort for the present simulations, an L-shaped wave function expansion scheme is employed for R and r degrees of freedom (they are defined in Fig. 1). For the reactions $H_2+NH_2/ND_2/NHD$, 70 grid points were used for R degree in a range of [2.0,12.0] a.u., and 30 grid points were used in the interaction region. For the breaking bond degree r , 25 and 5 vibrational basis functions were used in the interaction region and in the asymptotic region, respectively. For the two Radau radial coordinates, R_1 and R_2 , 3 PODVR vibrational basis functions were used for each of them. Eight PODVR functions were used for the θ degree in the nonreactive subgroup $NH_2/ND_2/NHD$. For the rotational basis functions, we used $j_{1max} = 24$ for H_2 , j_{2max} and $k_{max}=15$ for the nonreactive amino radical, which results in a total number of 99,709 functions for $J_{tot}=0$ by including the symmetry of H_2 . When H_2 is replaced by D_2 or HD , the total number of grid points for R is equal to 86 in including 33 grid points in the interaction region. The number of basis functions for r is also increased: 30 functions in the interaction region. The value of j_{1max} is equal to 28 and the number of rotational basis functions are equal to 122,091 and 238,579, for the reaction D_2+NH_2 and $HD+NH_2$, respectively.

Due to the large computational efforts in the coupled-channel (CC) calculations, which include all the K -block for different J_{tot} , the centrifugal-sudden (CS) approximation was applied in this work. Under the CS approximation, K (the projection of total angular momentum on the body-fixed z axis) is a good quantum number and the couplings between different K are neglected. In the previous studies for the atom-polyatomic reactions such as $H+H_2O$ and $H+CHD_3$, it has been shown that the CS approximation underestimates integral cross sections (ICSs) **Fabien: Ref.** On the contrary, for bimolecular reactions such as H_2+OH and H_2+NH_2 , the CS approximation leads to results close to the exact CC calculations **Fabien: Ref.** Keeping this in mind, we think that the CS approximation employed in this study is suitable and can give very reasonable results. Extensive calculations, where the total angular momentum J_{tot} was increased up to 80, were carried out to yield CS ICSs starting from the ground state and several vibrationally excited initial states for the five reactions.

In order to carry out the scattering calculations, one first needs to obtain the initial vibrational

states for the reagents. Table I lists the vibrational energies for the reactants $\text{NH}_2/\text{ND}_2/\text{NHD}$. (010) and (020) denote the first and second bending excitation states. For NH_2/ND_2 , (100) and (001) denote the first symmetric stretching excitation state and first antisymmetric stretching excitation state. For the NHD molecular system, (100) denotes the fundamental of the stretching mode of ND while (001) denotes the fundamental of the stretching mode of NH.

Mode selectivity is of great important in elemental chemical reactions. We will first examine how the excitation of vibrational modes for the three different reagents $\text{NH}_2/\text{NHD}/\text{ND}_2$ change the reactions with H_2 initially in its ground state. For the sake of clarity, we will present the results for the excitation of the same type of vibrational mode on the same figure. In this paper, the total energy is given relative to the ground state energy for the two reactants. Fig. IV gives the total reaction probabilities as a function of total energy for the $\text{NH}_2/\text{NHD}/\text{ND}_2$ initially in their ground states and after bending excitations for $J_{\text{tot}} = 0$. Globally, the ICS curves for these three initial states increase monotonously in the energy region of interest. For the $\text{NH}_2/\text{NHD}/\text{ND}_2$ ground state (000), as shown in Fig. 2 (a), the energy threshold for the three reactions is almost the same (about 0.43 eV). According to the *abinitio* calculations, the energy barrier for the $\text{H}_2 + \text{NH}_2 \rightarrow \text{H} + \text{NH}_3$ is about 0.414 eV. If one takes into account the zero point energies (ZPE) of the reactants, the ZPE corrected barrier height will be around 0.489 eV, 0.464 eV and 0.476 eV for the reactions $\text{H}_2 + \text{NH}_2$, $\text{H}_2 + \text{ND}_2$ and $\text{H}_2 + \text{NHD}$, respectively. Apparently, the tunneling effect for the $\text{H}_2 + \text{NH}_2$ is the strongest and for the $\text{H}_2 + \text{ND}_2$ is the weakest. With the increase of the energy, the ICS for the $\text{H}_2 + \text{NH}_2$ becomes the largest, reaches a value of $4 a_0^2$ at the energy $E = 1.47$ eV. At the same energy, NH_2 is the lightest among the three amino isotopologues and it moves faster than the other two with respect to H_2 . The differences of ICSs for there three reactions in the high energy region is apparently due to the fact that the product NH_3 moves the fastest and NHD_2 moves the slowest compared to others during the collision with the incoming H_2 molecule.

Fig. 2 also depicts the ICSs for excitation of the bending vibrational mode for the $\text{H}_2 + \text{NH}_2/\text{NHD}/\text{ND}_2$ reactions. For the first bending excitation states (010) of $\text{NH}_2/\text{NHD}/\text{ND}_2$, the curves for the three reactions show the same trends as for the ground state. A closer look at the low energy regions shows that there is a crossing point for the three curves at total energy of 0.87 eV (Fig. 2 (b)). While for the first overtone of the bending excitation states (020), the crossing point for the three curves becomes higher, around $E = 1.4$ eV (Fig. 2 (c)). In Figs. 2 (b) or 2 (c), the ICS for the reaction $\text{H}_2 + \text{ND}_2$ is the largest from the threshold to the crossing point, while the reaction $\text{H}_2 + \text{NH}_2$ is the lowest in the same energy region. When the energy is higher than the crossing point, the re-

sults are reversed. As can be seen in the Table I, the vibrational energies for the bending excitation states for ND_2 are the lowest because of the two heavy atoms D in ND_2 . In contrast, the vibrational energies for NH_2 are the highest for the two light H atoms. When compared with the results of the ground states of the three reactions, the results for the bending excitation modes of reagents as shown in Fig. 2 can be understood naturally. Moreover, one can see that the curves for the three reactions increase monotonously in the whole energy region. If the bending vibrational energies for the initial reactants are excluded from the total energy, one can find that the bending modes have little effect on the reactivity for each reaction. This conclusion is in agreement with the predictions of SVP (Sudden Vector Projection) model as well as the results of Song et.al **Fabien: Ref.**

In Fig. 3, we present the ICSs for the stretching excitation modes for initial reagents $\text{NH}_2/\text{NHD}/\text{ND}_2$. There are two results for the reaction H_2+NHD that are given in Fig. 3 (a) and 3 (b) since there are two different localized stretching vibrational modes. By visual inspection of these figures, we clearly see that when the reagent NHD is initially in ND stretching excitation mode (100), the reactivity will be the largest in the whole energy region. While when the initial energy is in the initial NHD stretching state (001), the enhancement on the reactivity is the lowest. One can understand this finding easily by attributing it to the fact that the vibrational energy ND (100) is much lower than for NH (001) in the NHD molecule (see Table I). For the two stretching excitation modes, the thresholds for the reaction H_2+NH_2 are almost the same as for the reaction H_2+NHD starting from (001). In contrast, the thresholds of the reaction H_2+ND_2 are very close to the reaction H_2+NHD starting from (100). Whereas the stretching excited energies for NH_2 and ND_2 are close to the vibrational energies NHD (001) and NHD (100), respectively. It is thus very natural to obtain these results. In Fig. 3 (a) and 3 (b), there also exist crossing points for the ICS curves for the reactions H_2+NH_2 and H_2+ND_2 which are similar to what we observed in the Fig. 2 (a) and 2 (b) for the reagents $\text{NH}_2/\text{ND}_2/\text{NHD}$ with initial excitations in the bending excitation states. Likewise, the behaviors for these results can be explained simply as follows: in the low energy region, the total energy deposited in the vibrational modes involving the D atoms (ND_2) induces larger reactivities because of its lower vibrational energy comparing with NH_2 , while in high energy region the heavier product ($m(\text{NHD}_2) > m(\text{NH}_3)$) leads to a lower velocity and reduces the reactivity.

Finally, when we look at Fig. 3 (a) and 3 (b) together, one can see that the two figures are very similar except that there is a small energy shift. The bond lengths of the NH or ND in the

nonreactive group $\text{NH}_2/\text{ND}_2/\text{NHD}$ are equal to $1.937 a_0$ and $1.936 a_0$ for the reagent and transition state, respectively. As in the previous studies performed by Yang et.al. **Fabien: Ref**, the seven-dimensional model by fixing the two NH bonds in NH_2 , which is called the spectator-bond approximation, agrees well with the full dimensional results. Herein, our results for the three isotopic reactions have clearly shown that the initial stretching excited of the reagent $\text{NH}_2/\text{ND}_2/\text{NHD}$ has little effect on the reactivity for each reaction.

Next, we investigate the isotope effects for the reagent hydrogen molecule, i.e., $\text{H}_2/\text{D}_2/\text{HD}+\text{NH}_2$. Fig. 4 shows the ICSs for the reaction $\text{H}_2/\text{D}_2/\text{HD}+\text{NH}_2(\nu_1=0,1) + \text{NH}_2(000)$ as a function of total energy. For the reaction $\text{H}_2/\text{D}_2+\text{NH}_2$, the values of ICSs have been divided by 2 because of the H_2/D_2 symmetry. While for the reaction $\text{HD}+\text{NH}_2$, there exist two reaction channels and the product can be either $\text{H}+\text{NDH}_2$ or $\text{D}+\text{NH}_3$. The coordinates for the reaction system, shown in Fig. 1, allow us to distinguish clearly the two reaction channels thanks to the coordinate θ_1 . In our calculations, the θ_1 is about equal to 17° at the NH_4 saddle point. When the H atom is replaced by the D atom, the flux that contributes to the NDH_2 product will be characterized by small values of θ_1 corresponding to configurations in which the D and N atoms are facing each other to form the NDH_2 product. In contrast, the flux characterized by large values of θ_1 corresponds to configurations in which the H atom is facing the N atom to form the product NH_3 . We see that strong steric effect exist in the $\text{HD}+\text{NH}_2$ reaction.

In Fig. 4 (a), the ICSs for the reaction H_2+NH_2 and D_2+NH_2 are very close and the energy threshold for D_2+NH_2 is slightly higher. The curves for the reaction $\text{HD}+\text{NH}_2$ show that the $\text{H}+\text{NDH}_2$ product channel is favored. This result is similar what is observed for the $\text{HD}+\text{OH}$ reaction. Overall, the four curves increase steadily with the increase of the energy. At the total energy of $E = 1.4 \text{ eV}$, the value of ICS for the reaction $\text{HD}+\text{NH}_2 \rightarrow \text{H}+\text{NDH}_2$ is about $2.52 a_0^2$ and the ICS for the reaction $\text{HD}+\text{NH}_2 \rightarrow \text{D}+\text{NH}_3$ is about $1.18 a_0^2$. When comparing with the ICSs for the reaction H_2+NH_2 and D_2+NH_2 , the average of the two channels for the reaction $\text{HD}+\text{NH}_2$ is also very close to these values. When the reagents $\text{H}_2/\text{D}_2+\text{NH}_2$ are initially excited starting from the $\nu = 1$ state, the reactivities for all the reactions are enhanced significantly as shown in Fig. 4 (b). When giving comparisons between Fig. 4 (a) and 4 (b), we found that the threshold energies for the ground state ($\nu_1 = 0$) are lower than the excited state ($\nu_1=1$) which indicates that the total energy deposited in translational energy is more effective on the reactivity than the initial $\text{H}_2/\text{D}_2/\text{HD}$ vibrational energy in the low total energy region.

Since there exist two channels for the reaction $\text{HD}+\text{NH}_2$, we give the branching ratio of the

ICSs between the two products $\text{H}+\text{NDH}_2$ and $\text{D}+\text{NH}_3$ for the reagent HD initially in two different states ($\nu_1=0$ and 1): they are as shown in Fig. 5. The two curves rise sharply in the low energy region then continue smoothly with the increase of total energy. Apparently, the ratio for the reaction channel HD initially in its ground state is larger than for the channel with HD initially in an excited state in the given energy region. In addition, for the HD ($\nu_1 = 0$) initial ground state, there is a peak around the total energy at $E = 0.53$ eV. Specifically, in the very low energy region the $\text{D}+\text{NH}_3$ product is dominant because of stronger tunneling effect involving the H atom in the reagent HD for the two channels. While at high energies, the D-transfer reaction channel is much more effective than the H-transfer reaction channel. The similar feature on the ratio were also observed in the reaction $\text{HD}+\text{OH}\rightarrow\text{H}+\text{HOD}/\text{D}+\text{H}_2\text{O}$.

IV. SUMMARY

A full dimensional study has been carried out for the reactions $\text{H}_2+\text{NH}_2/\text{ND}_2/\text{NHD}$ and $\text{H}_2/\text{D}_2/\text{HD}+\text{NH}_2$ based on a description of a combination of Jacobi and Radau coordinates. As in our previous studies on $\text{H}+\text{NH}_3$ and $\text{H}+\text{CH}_3$, Radau coordinates were used for the nonreactive moiety $\text{NH}_2/\text{ND}_2/\text{NHD}$ and PODVR basis functions are used to save the computational efforts. Our principal aim in this work is to study the isotope effects. For this, we performed extensive calculations describing the effects on the reactivities of the vibrational excitation of the two reagents and for their isotopologues. For the reagents $\text{NH}_2/\text{ND}_2/\text{NHD}$ initially in ground state, the ICS for the reaction $\text{H}_2(\nu=0)+\text{NH}_2$ gives rise to the largest ICS and the reaction $\text{H}_2(\nu=0)+\text{ND}_2$ is the lowest in the high energy region. When the reagent amino is initially in excited states, the vibrational modes exciting involving N-D will lead to lower thresholds than the vibrational modes excitation involving N-H. The behaviors in the threshold region are mainly attributed to the differences of the vibrational energies of the modes involving N-H or N-D. Generally speaking, the energy deposited in the $\text{NH}_2/\text{ND}_2/\text{NHD}$ bending or stretching modes is less efficient in promoting reactivity than translational energy for the reactions. For the reactions $\text{H}_2/\text{D}_2/\text{HD}+\text{NH}_2$, the energy deposited in the $\text{H}_2/\text{D}_2/\text{HD}$ vibrational excitation will inhibit the reactivities in the lower energy region but enhances the reactivities in the high energy region. The reaction $\text{D}_2(\nu_1=1)+\text{NH}_2(000)$ possesses the lowest threshold energy due to its lowest vibrational excitation energy. The tunneling and steric effects play important role in the reaction $\text{HD}+\text{NH}_2$ since it contains two competitive product channels.

Data Availability Statement The data that support the findings of this study are available from the corresponding author upon reasonable request.

Acknowledgments The project was supported by the National Natural Science Foundation of China (Nos. 21433009, 21688102, and 21703243), the Chinese Academy of Sciences(Grant No. XDB17010000). F.G. thanks “French Chinese Network in Theoretical Chemistry” (GDRI 0808) for financial support.

REFERENCES

- ¹X. Wang, W. Dong, C. Xiao, L. Che, Z. Ren, D. Dai, X. Wang, P. Casavecchia, X. Yang, B. Jiang, D. Xie, Z. Sun, S.-Y. Lee, D. H. Zhang, H.-J. Werner, and M. H. Alexander, *Science*. **322**, 573 (2008).
- ²W. Dong, C. Xiao, T. Wang, D. Dai, X. Yang, and D. H. Zhang, *Science*. **327**, 1501 (2010).
- ³C. Xiao, X. Xu, S. Liu, T. Wang, W. Dong, T. Yang, Z. Sun, D. Dai, X. Xu, D. H. Zhang, and X. Yang, *Science*. **333**, 440 (2011).
- ⁴T. Wang, J. Chen, T. Yang, C. Xiao, Z. Sun, L. Huang, D. Dai, X. Yang, and D. H. Zhang, *Science*. **342**, 1499 (2013).
- ⁵T. Yang, J. Chen, L. Huang, T. Wang, C. Xiao, Z. Sun, D. Dai, X. Yang, and D. H. Zhang, *Science*. **347**, 60 (2015).
- ⁶S. Liu and D. H. Zhang, *Chem. Sci.* (2015).
- ⁷D. Yuan, Y. Guan, W. Chen, H. Zhao, S. Yu, C. Luo, Y. Tan, T. Xie, X. Wang, Z. Sun, D. H. Zhang, and X. Yang, *Science* **362**, 1289 (2018).
- ⁸B. Jiang and H. Guo, *J. Am. Chem. Soc.* **135**, 15251 (2013).
- ⁹J. Li, B. Jiang, and H. Guo, *J. Am. Chem. Soc.* **135**, 982 (2013).
- ¹⁰J. Li, B. Jiang, H. Song, J. Ma, B. Zhao, R. Dawes, and H. Guo, *J. Phys. Chem. A*. **119**, 4667 (2015).
- ¹¹X. Zhang, L. Li, J. Chen, S. Liu, and D. H. Zhang, *Nat. Commun.* **11**, 223 (2020).
- ¹²Z. Sun, B. Zhao, S. Liu, and D.-H. Zhang, in *Molecular Quantum Dynamics*, edited by F. Gatti (Springer, Heidelberg, 2014).
- ¹³M. Qiu, Z. Ren, L. Che, D. Dai, S. A. Harich, X. Wang, X. Yang, C. Xu, D. Xie, M. Gustafsson, R. T. Skoedje, Z. Sun, and D.-H. Zhang, *Science* **311**, 1440 (2006).
- ¹⁴J. Palma and D. C. Clary, *J. Chem. Phys.* **112**, 1859 (2000).

- ¹⁵L. Zhang, Y. Lu, S.-Y. Lee, and D. H. Zhang, J. Chem. Phys. **127**, 234313 (2007).
- ¹⁶S. Liu, J. Chen, Z. J. Zhang, and D. H. Zhang, J. Chem. Phys. **138**, 011101 (2013).
- ¹⁷Y. Zhou and D. H. Zhang, J. Chem. Phys. **141**, 194307 (2014).
- ¹⁸Z. Zhao, Z. Zhang, S. Liu, and D. H. Zhang, Nat. Commun. **8**, 14506 (2017).
- ¹⁹Y. Zhou, C. R. Wang, and D. H. Zhang, J. Chem. Phys. **135**, 024313 (2011).
- ²⁰Z. Zhang and D. H. Zhang, J. Chem. Phys. **141**, 144309 (2014).
- ²¹R. Liu, M. Yang, G. Czako, J. M. Bowman, J. Li, and H. Guo, J. Phys. Chem. Lett. **3**, 3776 (2012).
- ²²Z. J. Zhang, Y. Zhou, D. H. Zhang, G. Czako, and J. M. Bowman, J. Phys. Chem. Lett. **3**, 3416 (2012).
- ²³R. Liu, F. Y. Wang, B. Jiang, G. Czako, M. H. Yang, K. P. Liu, and H. Guo, J. Chem. Phys. **141**, 9 (2014).
- ²⁴N. Liu and M. Yang, J. Chem. Phys. **143**, 134305 (2015).
- ²⁵J. Qi, H. Song, M. Yang, J. Palma, U. Manthe, and H. Guo, J. Chem. Phys. **144**, 171101 (2016).
- ²⁶J. Chen, X. Xu, S. Liu, and D. H. Zhang, Phys. Chem. Chem. Phys. **20**, 9090 (2018).
- ²⁷W. Q. Zhang, Y. Zhou, G. R. Wu, Y. P. Lu, H. L. Pan, B. N. Fu, Q. A. Shuai, L. Liu, S. Liu, L. L. Zhang, B. Jiang, D. X. Dai, S. Y. Lee, Z. Xie, B. J. Braams, J. M. Bowman, M. A. Collins, D. H. Zhang, and X. M. Yang, Proc. Natl. Acad. Sci. U.S.A. **107**, 12782 (2010).
- ²⁸R. van Harreveld, G. Nyman, and U. Manthe, J. Chem. Phys. **126**, 084303 (2007).
- ²⁹F. Huarte-Larrañaga and U. Manthe, J. Chem. Phys. **113**, 5115 (2000).
- ³⁰F. Huarte-Larrañaga and U. Manthe, J. Phys. Chem. A **105**, 2522 (2001).
- ³¹F. Huarte-Larrañaga and U. Manthe, J. Chem. Phys. **116**, 2863 (2002).
- ³²G. Schiffel and U. Manthe, J. Chem. Phys. **132**, 191101 (2010).
- ³³R. Welsch and U. Manthe, J. Chem. Phys. **137**, 244106 (2012).
- ³⁴R. Welsch and U. Manthe, J. Chem. Phys. **138**, 164118 (2013).
- ³⁵R. Welsch and U. Manthe, J. Chem. Phys. **141**, 051102 (2014).
- ³⁶R. Welsch and U. Manthe, J. Chem. Phys. **141**, 174313 (2014).
- ³⁷R. Welsch and U. Manthe, J. Chem. Phys. **142**, 064309 (2015).
- ³⁸T. Wu and U. Manthe, J. Chem. Phys. **119**, 14 (2003).
- ³⁹T. Wu, H.-J. Werner, and U. Manthe, J. Chem. Phys. **124**, 164307 (2006).
- ⁴⁰Z. Zhang, F. Gatti, and D. H. Zhang, J. Chem. Phys. **150**, 204301 (2019).
- ⁴¹Z. Zhang, F. Gatti, and D. H. Zhang, J. Chem. Phys. **152**, 201101 (2020).

- ⁴²J. Echave and D. C. Clary, Chem. Phys. Lett. **190**, 225 (1992).
- ⁴³H. Wei and T. Carrington Jr., J. Chem. Phys. **97**, 3029 (1992).
- ⁴⁴R. Radau, Annales Scientifiques de l'Ecole Normale Supérieure **5**, 311 (1868).
- ⁴⁵F. T. Smith, Physical Review Letters **45**, 1157 (1980).
- ⁴⁶M. J. Bramley and T. Carrington, Jr., J. Chem. Phys. **99**, 8519 (1993).
- ⁴⁷F. Gatti, C. Iung, M. Menou, Y. Justum, A. Nauts, and X. Chapuisat, J. Chem. Phys. **108**, 8804 (1998).
- ⁴⁸F. Gatti, C. Iung, M. Menou, and X. Chapuisat, J. Chem. Phys. **108**, 8821 (1998).
- ⁴⁹F. Gatti and C. Iung, Phys. Rep. **484**, 1 (2009).
- ⁵⁰G. Brocks, A. V. D. Avoird, B. T. Sutcliffe, and J. Tennyson, Mol. Phys. **50**, 1025 (1983).
- ⁵¹C. Leforestier, R. H. Bisseling, C. Cerjan, M. D. Feit, R. Friesner, A. Guldenberg, A. Hammerich, G. Jolicard, W. Karrlein, H.-D. Meyer, N. Lipkin, O. Roncero, and R. Kosloff, J. Comp. Phys. **94**, 59 (1991).

TABLE I. Vibrational energies for $j_2 = 0$ (without rotation) levels (in cm^{-1}) for NH_2 , ND_2 and NHD .

State	NH_2	ND_2	NHD
(010)	1501.80	1113.86	1323.73
(020)	2965.35	2205.92	2621.14
(100)	3215.68	2358.55	2400.85
(001)	3292.50	2455.28	3256.55

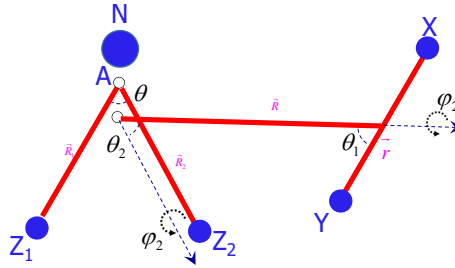


FIG. 1. The Jacobi and Radau vectors for the $XY+NZ_{1,2}$ system. A is the “canonical” point of $NZ_{1,2}$, G is the center mass of the $NZ_{1,2}$. \vec{R}_1 and \vec{R}_2 are the Radau vectors. \vec{R} and \vec{r} are two Jacobi vectors.

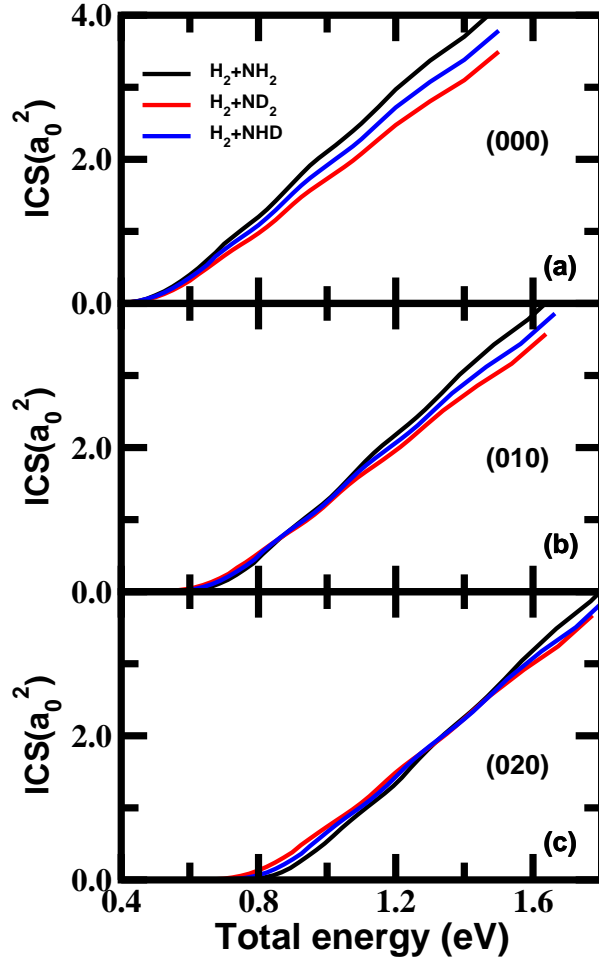


FIG. 2. The integral cross sections for the reactions $H_2 + NH_2/ND_2/NHD(\nu_1\nu_2\nu_3)$ as a function of total energy. (a) The reagents $NH_2/ND_2/NHD$ initially in their vibrational ground state (000). (b) Same as (a) but starting from the first bending excited states (010). (c) Same as (a) but starting from the second bending excited states (020).

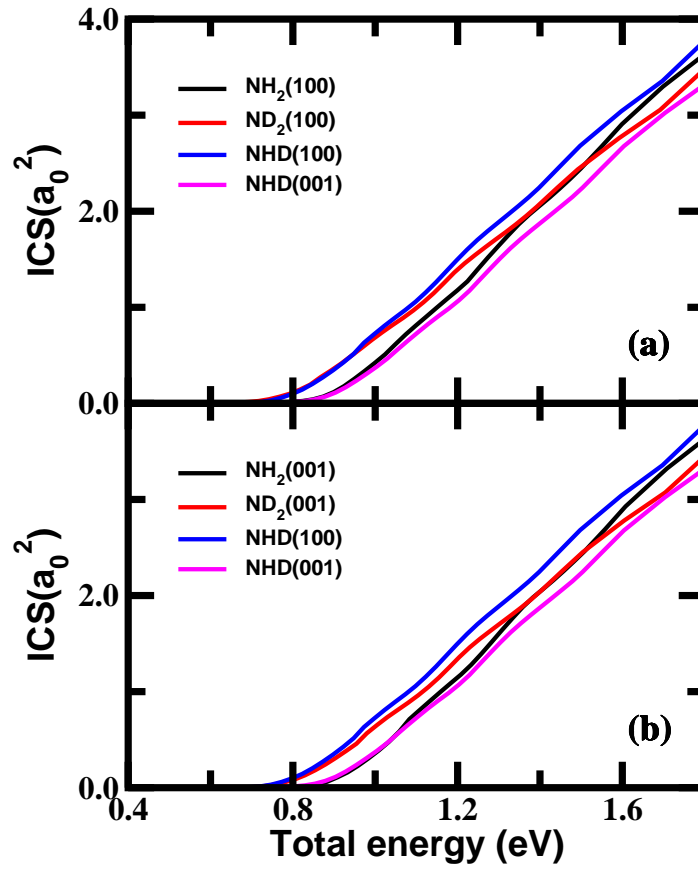


FIG. 3. Same as Fig. 2 but for first stretching excited states (100) and (001).

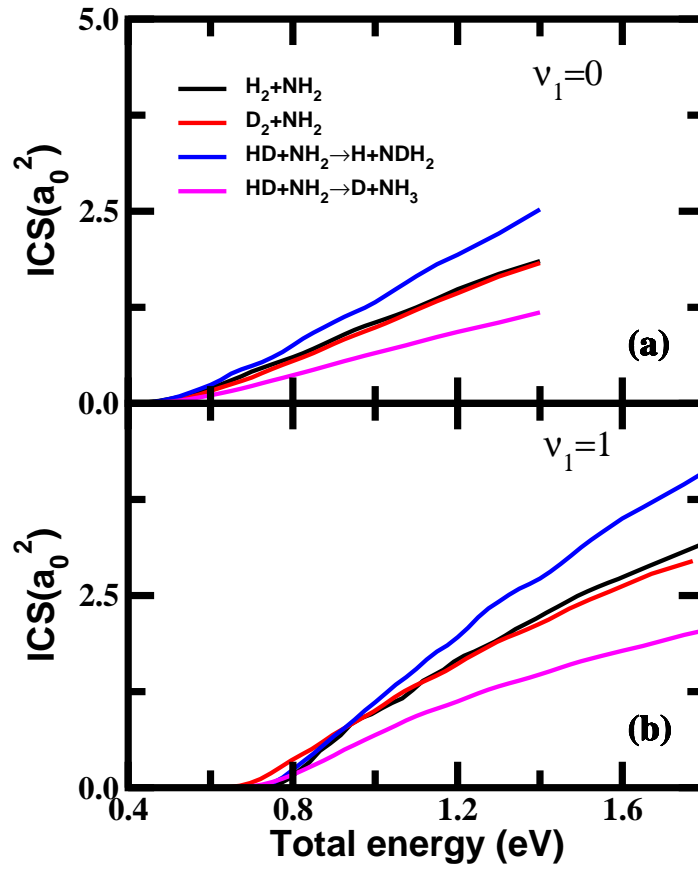


FIG. 4. The integral cross sections for the reactions $\text{H}_2/\text{D}_2/\text{HD}+\text{NH}_2$ as a function of total energy and the values for the reactions $\text{H}_2/\text{D}_2+\text{NH}_2$ are divided by a factor of 2. (a) The reagents $\text{H}_2/\text{D}_2/\text{HD}$ initially in their ground states ($\nu_1=0$). (b) Same as (a) but starting from the first excited states ($\nu_1 = 1$)

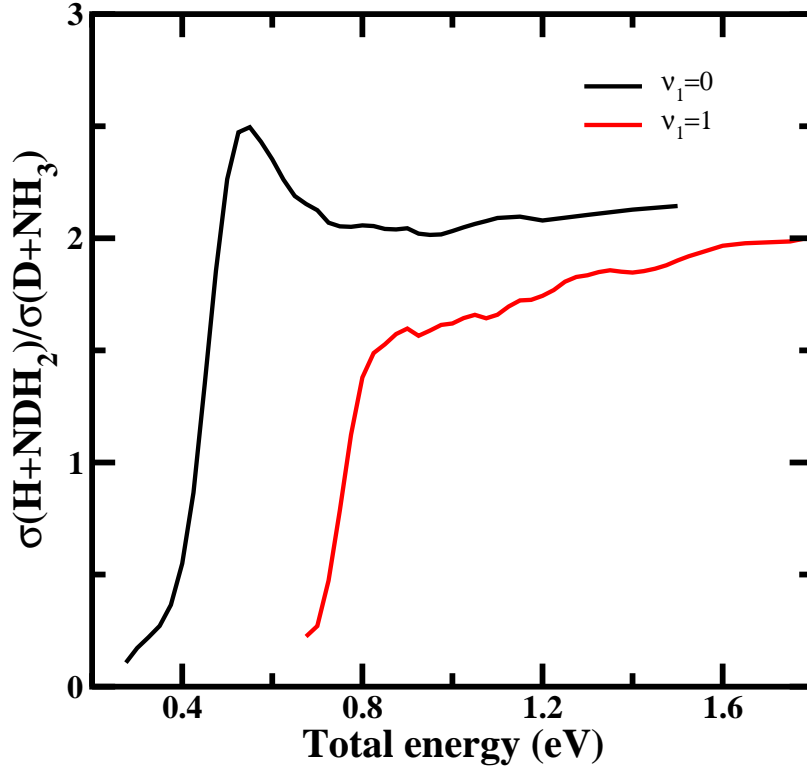


FIG. 5. Branching ratio for the reactions $\text{HD}(\nu_1 = 0, 1) + \text{NH}_2 \rightarrow \text{H} + \text{NDH}_2$ and $\text{HD}(\nu_1 = 1, 2) + \text{NH}_2 \rightarrow \text{D} + \text{NH}_3$.